Bull. Mater. Sci., Vol. 24, No. 2, April 2001, pp. 111–116. © Indian Academy of Sciences.

Fracture resistance of 8 mol% yttria stabilized zirconia

B F SORENSEN and A N KUMAR*

*Indian Institute of Technology, Hauz Khas, New Delhi 110 016, India
Riso National Laboratory, DK 4000, Roskilde, Denmark

Abstract. An *in situ* technique for the assessment of fracture resistance employing double cantilever beam (DCB) specimens was developed in the present study. The side-grooved DCB specimens were loaded with pure bending moments in a specially designed and fabricated test fixture which went inside the specimen chamber of a scanning electron microscope. The study as conducted on a 8 mol% fully stabilized cubic phase yttria (Y_2O_3) stabilized zirconia (YSZ) ceramic. The powder processed sheets were sintered at 1600°C for 2 h in a zirconia tube furnace. The mode I applied energy release rate, G_I was determined for both pure YSZ and treated YSZ. Two sets of experiments were conducted for the complete characterization of the ceramics. Three fracture toughness values were determined for the pure and treated ceramics, viz. (i) at the onset of the crack initiation, G_{ic}, (ii) at the arrest of a subcritical crack, G_{ia} and (iii) at the onset of the fast fracture, G_{if}. Two analyses of the experimental data were carried out, viz. method of extrapolation and statistical analysis. In case of the pure YSZ, a transgranular mode of the stable crack growth was identified to be predominant. The porous coating treatment appeared to have positive effects as the crack initiation resistance increased due to electrode layers. The stable crack growth behaviours of the ceramics were investigated by monitoring the crack growth velocity as a function of applied *G* values. The results obtained were of direct significance in designing and fabrication of SOFC stacks.

Keywords. YSZ; fracture resistance; fracture energy; fracture toughness; SOFC stacks.

1. Introduction

A high fracture toughness of the structural materials is recognized to be an essential property to achieve safety and integrity. Brittle materials, in particular ceramics, often possess a low fracture toughness value which limits their engineering applications (Anderson 1995). In recent times, the development of a technology for a solid oxide fuel cell (SOFC) for electricity generation has placed as a demand on a special variety of ceramics, like, dense 8 mol% yttria stabilized zirconia (YSZ) as electrolyte (Steele 1994; Larsen *et al* 1995). These are used as electrolyte sheets coated with porous electrode layers on either side, viz. Ni–ZrO_2 cermet as anode and stonsium doped lanthanum manganite ($LaSrMnO_3$) as cathode. The cells comprising of three layers are separated by an interconnect made of doped lanthanum chromite ($LaCrO_3$). A large thermal residual stress exists in the layers mainly due to the differences in the thermal expansion coefficients (TEC) and stiffness values (Larsen *et al* 1995). The SOFC must be designed to sustain on and off thermal cycling without cracking that degrades the functional performance of the cell. The need for a sufficiently high fracture toughness for those ceramics is, therefore, essentially to prevent a premature failure and sustain the structural integrity during its operation. However, measuring fracture toughness data in ceramics still remains a difficult task and a standard universal technique is not yet established (Sakai and Bradt 1993; Ponton and Rawlings 1989). Stable crack growth is necessary to obtain a reliable and unambiguous fracture toughness data. In a recent work, the authors have proposed an *in situ* method employing double cantilever beam (DCB) specimens (Kumar and Sorensen 1999) to measure the fracture toughness property. The method is to load a DCB specimen with pure bending moments. The method is capable of generating stable crack growth under various environmental conditions. The controlled crack growth was studied inside the vacuum chamber of the environmental scanning electron microscope (ESEM). This allows an adaptation of an *in situ* crack propagation observed simultaneously at high magnification and resolution. Details of the technique and the key advantages for studying stable cracking in ceramics are outlined elsewhere (Sorensen *et al* 1998).

Since there has been an adequate information on the fracture resistance property of YSZ and insufficient data for the mechanical design, attempt has been made to investigate the fracture resistance behaviour of the ceramics components i.e. pure (monolithic) YSZ for application in SOFC.

2. Experimental

2.1 *Pure YSZ*

Bars of around 5 mm in thickness were made from 8 mol% fully stabilized cubic YSZ (TZ-8Y, Tosoh Co.,

*Author for correspondence

Japan) powder using uniaxial pressing at room temperature. The bars were then isostatically pressed at 3400 bars to achieve high density in excess of 98%. Sintering of YSZ bars was done at 1600°C for 2 h in a clean zirconia tube furnace.

2.2 *Specimen geometry and loading*

A double cantilever beam (DCB) specimen with a single side-groove was used for study. The notch configuration in the specimen with the dimensions is shown in figure 1. The pure YSZ bars prepared as above were machined with diamond tools to obtain flat chevron notched DCB type specimen with a groove on one side only. The loading arrangement was pure bending moments at the beams of the specimen under rotation control (Kumar and Sorensen 1999). A LVDT was attached to the fixture mouth to record the relationship between applied bending moment and opening displacement. It was also possible to record the extent of crack growth as a function of time. All coating treatments were imparted on the specimen surfaces. The plane surface of the DCB specimens was initially polished to 4 μ level using diamond paste. The specimen geometry, dimensions, groove size, etc are similar to those reported in an earlier study (Sorensen *et al* 1998).

2.3 *YSZ coating*

The YSZ specimens were treated with four different coatings. The coatings were applied by slurry paintings at room temperature. Each specimen consisted of a coated and an uncoated part. The coatings were dried for over 24 h before sintering. The coating thickness was maintained between 50 and 60 μ in all cases. Sintering was carried out at 1300°C for 2 h. The heating and cooling rates were 100°C per hour to achieve a homogeneous temperature field throughout the specimen. Since each specimen contained both coated and uncoated parts, the fracture resistance in both the impure YSZ and coated regions could be determined for each DCB specimen. The coating materials applied were: anode coating with Ni-8 mol% YSZ cermet (55 vol.%) on the plane surface; anode coating with NiO and MnO_2 (2–3%) mixture on plane surface; cathode coating with lanthanum (0·85) strontium (0·15) manganite (LSM) on plane surface; and anode and cathode coating with Ni–YSZ and LSM on grooved surface and on plane surface.

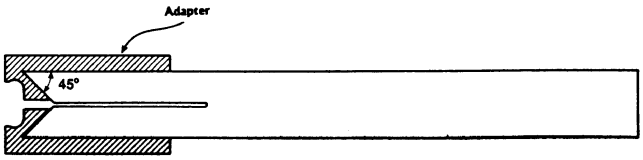

Figure 1. DCB specimen with steel loading fixture at the mouth.

2.4 *Experiments*

The polished DCB specimens were mounted on the specimen stage and inserted in ESEM to measure the room temperature fracture resistance. The details about the specimen mounting, test fixture, loading arrangement, instrumentation, sensing and monitoring of crack growth, computation of elastic energy release rate, etc were discussed in the earlier paper (Kumar and Sorensen 1999).

Two types of experiments were carried out on precracked specimens:

Type 1. The applied moment was monotonically increased at a slow, constant rate until crack growth just occurred from a stationary sharp crack. This was followed by a fast reduction in the moment to a low level (unloading) to arrest the crack. This (loading–unloading) cycle was repeated over 30–50 times on the same specimen. The test sequence is schematically shown in figure 2. The load at the onset of the crack growth and the corresponding crack front position before crack initiation (loading) and after crack arrest (unloading) were recorded for each loading–unloading cycle.

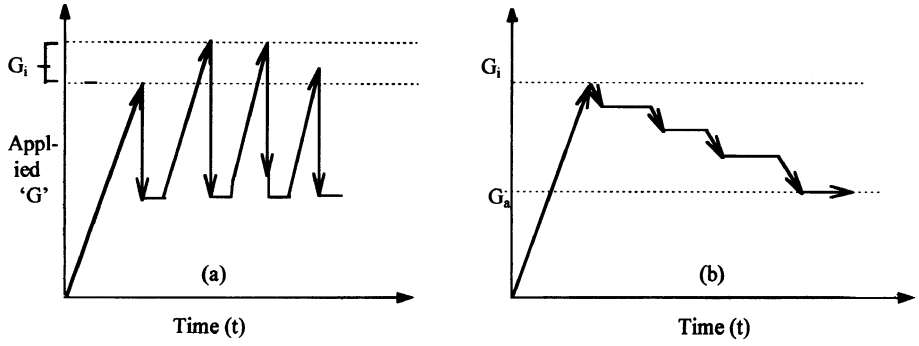

Figure 2. Schematic representation of test procedure. (**a**) Loading–unloading sequence for determination of G_i and (**b**) step unloading for determination of G_a.

Type 2. The crack growth was initiated as described in type 1. The crack growth was allowed to continue over some period (usually 10 to 12 min) under the fixed grip condition. This was followed by a decrease in load level on the specimen (partial unloading) by around 10% with respect to the previous load. Figure 2 illustrates the second set of experiments. Micrographs were taken at several stages during the crack propagation and crack arrest positions to reveal the mechanism(s) of cracking.

The process and mechanisms of crack growth in the treated specimens were further investigated by examining the fractured surfaces in ESEM (Kumar and Sorensen 1999).

3. Results

3.1 *Energy release rate (G)*

Mode I energy release rate (G) parameter was calculated using the following relation (Frieman *et al* 1995)

$$G = 12(1 - \nu^2)M^2/EBbH^3, \quad (1)$$

where M is the applied moment, B the specimen width, b the width of remaining ligament, H the beam height, E and ν are the Young's modulus and Poisson's ratio, respectively. If the bending moments, M are constant, the value of G remains constant, independent of the crack length. The loading arrangement thus allowed to conduct the experiments with crack propagation over a range of applied G.

3.2 *Fracture toughness (G_i)*

As G exceeded G_i (under monotonic loading condition), stable crack growth took place (figure 2). G_i values were determined by two methods. In the first case, statistical analysis comprising statistical mean (X) and standard deviation (s) was found with the population of the observed data. The G_i values as determined are given in table 1 for different conditions. The sample size considered for statistical estimation is also given in table 1.

In the second approach, the observed G_i values were plotted against the extent of crack growth (Δa) and time (t) as shown in figure 3. A somewhat conservative estimation of G_i is obtained by extrapolation of a linear plot made through the data points up to the x-axis where it is zero. This value was termed as G_i^0 and is included in table 1. The second set of experiments also allowed the measurement of the level of G at which the subcritical crack growth became dormant (crack arrest). The corresponding elastic energy release rate was termed as G_a. The determination of G_a by successive reduction of the moment is illustrated in figure 2b.

3.3 *Crack growth rate (*d*a/*d*t)*

The stable crack growth rate behaviour of the samples at $\leq G$ was studied from the type 2 experiments (figure 2). During the periods of crack growth (10–12 min) G was found to be decreasing marginally due to crack extension. An average of G was plotted against the corresponding crack growth velocity, which was obtained by averaging the total crack extension over the time of crack growth. Figures 4 and 5 show typical plots for crack growth kinetics. The crack growth behaviour was studied under the two loading conditions, viz. for $G = G_i$ (critical) and $G < G_i$ (subcritical). The average crack growth rate data is also included in table 1.

4. Discussion

4.1 *YSZ toughness*

The coating treatments appear to increase the initiation fracture toughness of YSZ to a varying degree as compared with the corresponding values for pure YSZ. The gain in the fracture initiation toughness, G_i was found to be maximum for NiO coating (around 55%) while it was around 30% in the case of NiO–MnO_2 mixture and NiO–LSM coatings. This improvement was also noticed in the values of G_a for NiO cermet coating (table 1). The improvement was quite significant. However, in case of NiO–LSM and NiO–MnO_2, there was no effect on the G_a values. The cracking behaviour is linearly represented by logarithmic relationship

Table 1. Fracture resistance and crack growth results for the treated and untreated YSZ.

Specimen condition ⇒ Measured data ⇓	Ni–YSZ cermet	NiO + MnO_2 mixture	NiO–YSZ + La–Sr–MnO_3	Pure YSZ (untreated)
Mean G value (G_i) and standard deviation at crack growth (J/m^2)	X = 5·48 0·21	X = 4·70 0·64	X = 4·46 0·32	X = 3·50 s = 0·17
Mean G value (G_i^0) (with extrapolation for $\Delta a \rightarrow 0$) (J/m^2)	5·35	4·54	4·29	3·47
Number of measurement	37	24	63	19
Experimental G values at crack arrest (G_a) (J/m^2)	3·7–3·9	2·9–3·00	2·75–2·90	–

$$du/dt = A(G_1)^n. \quad (2)$$

The values of the exponents in coated YSZ lies around 8–12 in comparison to the value of 11 for pure YSZ. In a recent work, Atkinson and Selcuk (1998) confirmed the susceptibility to such cracking in YSZ by the stress relaxation of double torsion specimen under constant displacement at ambient condition. The authors reported exponent values for crack growth rate lying around 20–22, based on the stress intensity factor parameter, K, in our work, G may be substituted by K in (2) to obtain

$$da/dt = A^{\#}(K)^m, \quad (3)$$

where, $A^{\#}$ is the new pre-exponential constant and $m = 2n$. The value of the exponent in the function becomes double when represented by a parameter K. The range of the exponent turns out to lie in the range 17–25 in the present work.

Mn diffusion from LSM and MnO_2 into YSZ resulted in a concentration gradient of Mn in the electrolyte.

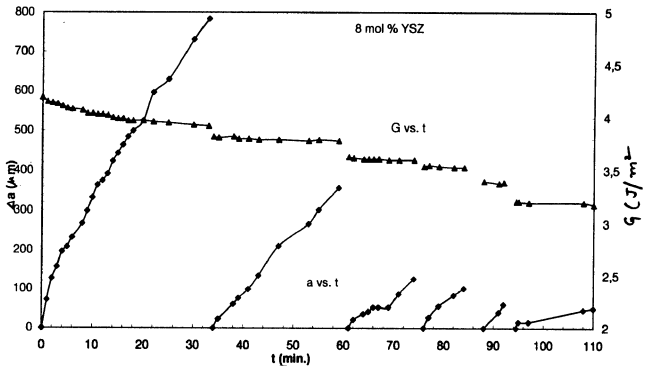

Figure 3. Changes in crack growth (Δa) and energy release rate (G) with time (t).

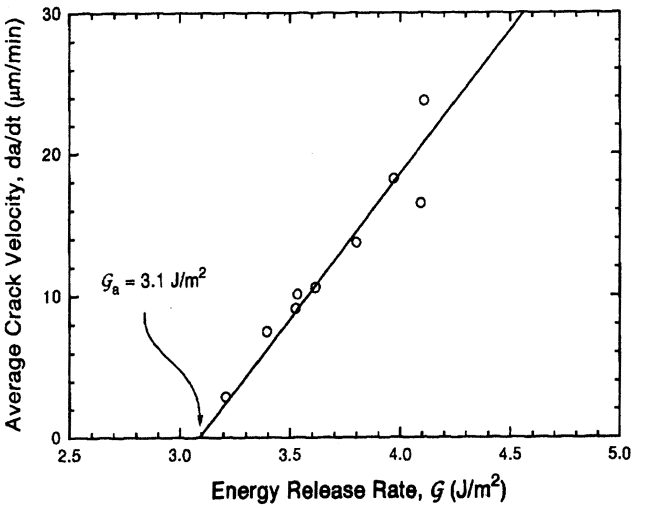

Figure 4. Crack velocity vs energy release rate (G) in pure YSZ.

The XRD studies showed the lattice size in zirconia to decrease with Mn content (Appel 1995), in particular when the Mn concentration was in excess of 5%. Interaction of NiO with YSZ was demonstrated to follow Arrhenius law (Kawada *et al* 1992; Taimatsu *et al* 1992; Kuzjukuvics and Linderoth 1997). The lattice contraction resulted in the tensile residual stresses on the surface layer of the treated YSZ. However, compressive stresses resulted in the remaining part of the thickness. The compressive zone in the YSZ was expected to be much larger in dimension than the region with the tensile stresses. On the other hand, the surface tensile stresses must have been much higher than the bulk compressive stresses, since the stresses must outbalance each other. This appears to contribute to the enhancement in the fracture energy in the YSZ treated with Mn and MnO_2.

4.2 *Stable crack growth mechanism*

The mechanisms of the crack growth in pure YSZ were discussed in detail in an earlier paper (Kumar and Sorensen 1999). Some representative micrographs revealing the cracking mechanisms in treated YSZ are displayed in figures 6–7. The crack growth in all treated specimens occurred by transgranular cracking mechanism. As the crack passed through the treated region and propagated into the pure YSZ region, it was seen to follow a transgranular path (figure 6). It was also possible to arrest the cracks within the grain by controlling the applied G value. The most interesting feature of the crack growth observed in coated YSZ was crack bridging. Quite frequently such regions could be found during its growth. Many times such bridging took place in series, but the direction of propagation was only deviated insignificantly from the pure mode I direction (figure 6). This indicated that the bridging was a localized phenomenon and was related with the microstructure. The applied G values associated with the regions of the crack bridging were found to be somewhat higher than the regions where no bridging took

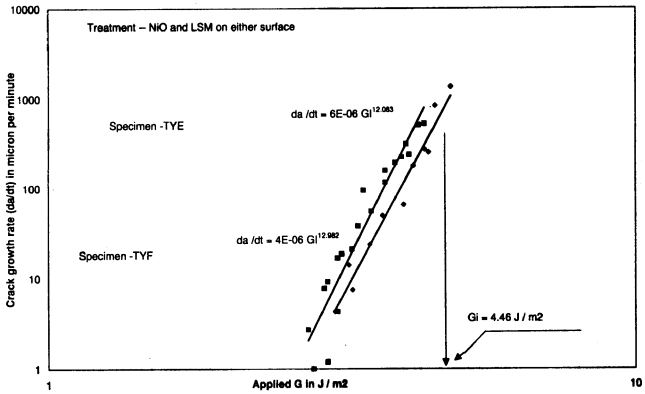

Figure 5. Crack velocity vs energy release rate (G) in surface treated YSZ.

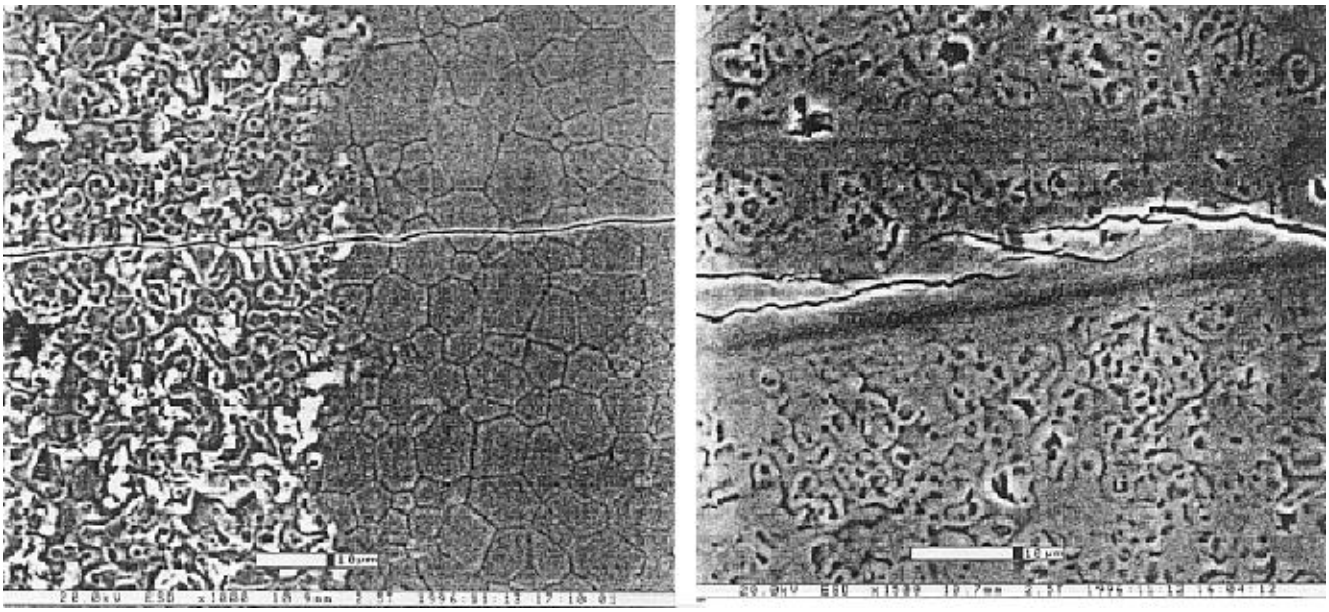

Figure 6. Typical micrographs showing the mechanism of crack propagation in YSZ.

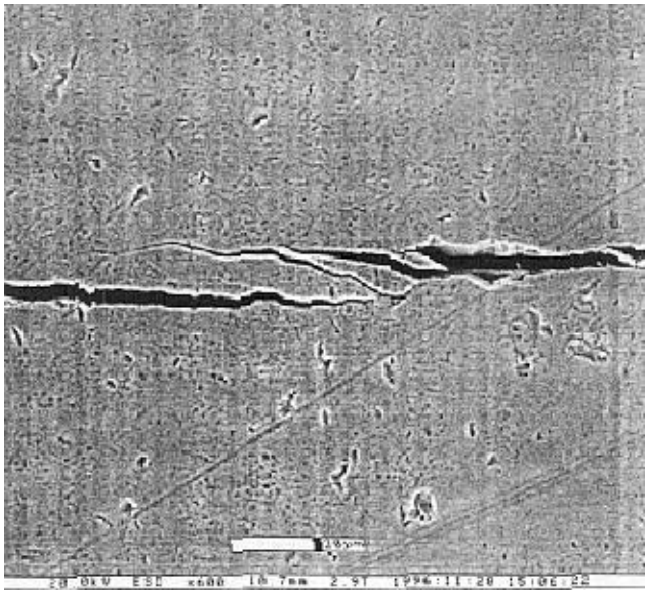

Figure 7. Typical micrograph showing the extent of crack bridging during its growth.

place. Crack bridging appeared to result from the diffusional effects during sintering and porous nature of the coated electrodes. In addition, grain bridging (where a crack grows around a single grain instead of cutting across the grain) also could be seen occasionally. Usually the crack propagated in a fairly straight manner. In case of coating with NiO and MnO_2 the crack appeared to propagate somewhat in a zigzag manner unlike the other cases. Phenomena like secondary cracking and branching were seldom observed in the surface treated YSZ specimens (figure 7).

5. Conclusions

(I) Three fracture toughness data emerged from the present work, viz. at crack initiation, at crack arrest and at fast (unstable) fracture. All three are needed for complete characterization of the crack resistance behaviour in ceramics. Significant enhancement in the fracture resistance behaviour of the surface treated YSZ from 3·5 to 5·48 J/m^2 are observed, the G_a value increased from 3·0 to 3·7–3·9 J/m^2 for pure YSZ. Interdiffusion of Mn and Ni from the coating during sintering appeared to introduce tensile residual stresses near the surface and low compressive stresses in the bulk of YSZ during sintering.

(II) The stable crack growth rate (da/dt) was observed to be a strong function of the applied elastic energy release rate, G and can be analytically represented by a logarithmic relationship of the form, $da/dt = A(G)^n$. The values of the exponents lie in the range 8–12 in all the cases. The crack growth rate was observed to have no insignificant effect by the surface treatment. The crack growth mechanism was predominantly transgranular in nature as in pure YSZ.

References

Anderson T L 1995 *Fracture: fundamental and application* (New York: Butterworths) 2nd ed

Appel C C 1995 *Ionics* **1** 406

Atkinson A and Selcuk A 1998 3*rd European solid oxide fuel cell forum* (ed.) P Stevens (Oberrohdorf, Switzerland: European SOFC Forum) p. 343

Kawada T, Sakai N, Yokokawa H, Dokiya M and Anzai I 1992 *Solid State Ionics* **50** 189

Kumar A N and Sorensen B F 2000 *J. Am. Ceram. Soc.* **83** 1199

Kuzjukuvics A and Linderoth S 1997 *Solid State Ionics* **93** 255

Larsen P H, Badgger C, Mogensen M and Larsen G 1995 *Proc. 4th European conf. on solid oxide fuel cell* (ed.) M Dokiya (Electrochemical Society) p. 69

Ponton C B and Rawlings R D 1989 *Mater. Sci. Engg*. **5** 865

Sakai M and Bradt R C 1993 *Int. Mater. Rev*. **38** 53

Sorensen B F, Horsewell A, Jorgensen O, Kumar A N and Engback P 1998 *J. Am. Ceram. Soc*. **81** 661

Steele B C H 1994 *Proc. 1st European SOFC Forum, Baden, Switzerland* (ed.) U Bossel **1** p. 375

Taimatsu H, Wada K, Kaneko H and Yamamura H 1992 *J. Am. Ceram. Soc*. **75** 401